25 May 2001

ELSEVIER

Chemical Physics Letters 340 (2001) 83–88

CHEMICAL PHYSICS LETTERS

www.elsevier.nl/locate/cplett

Controlling the branching ratio of the photodissociation of aligned Cl_2 at 404 nm

Akihiro Sugita [a], Kunihiro Suto [a,1], Masahiro Kawasaki [a,*], Yutaka Matsumi [b]

[a] *Department of Molecular Engineering, Kyoto University, Kyoto 606-8501, Japan*
[b] *Solar Terrestrial Environment Laboratory, Nagoya University, Toyokawa 442-8507, Japan*

Received 19 December 2000; in final form 20 March 2001

Abstract

Non-resonant infrared Nd^{3+}:YAG laser pulses at 1.06 μm were used to align chlorine molecules in a cold molecular beam. The degree of alignment was demonstrated by measurement of the velocity anisotropy of the photofragment $Cl(^2P_{3/2})$ atoms from $Cl_2(X^1\Sigma_g^+) + 404\ nm \rightarrow Cl_2(B^3\Pi_u^+, \Omega = 0) \rightarrow Cl(^2P_{3/2}) + Cl(^2P_{1/2})$. The branching ratio of the photoexcitation to $Cl_2(B^3\Pi_u^+, \Omega = 0)$ with respect to $Cl_2(^1\Pi_u, \Omega = 1)$ was controlled, allowing the selectivity of the two different adiabatic photodissociation channels: $Cl(^2P_{3/2}) + Cl(^2P_{1/2})$ and $Cl(^2P_{3/2}) + Cl(^2P_{3/2})$.

1. Introduction

Recent publications in the literature have demonstrated that active optical control of chemical reaction dynamics is possible by varying the optical phase of an ns laser pulse [1–3], shaping an ultrafast laser pulse [4], and aligning parent molecules by non-resonant infrared laser pulse [5]. Among them, the selective excitation is obtained by controlling the spatial alignment of the molecules with respect to the polarization of the exciting light so that either a parallel transition is enhanced and simultaneously a perpendicular transition suppressed or vice versa. A strong non-resonant laser field controls the alignment of the molecules since the interaction between the induced dipole moment of the molecules and the strong linearly polarized laser field forces the molecules to align along the polarization axis [6–9]. Parker and his co-workers [10–12] reported in their one-color photodissociation of CH_3I, O_2 and H_2 that the alignment effect caused by an ultrafast intense dissociating laser pulse increases the parallel angular anisotropy parameter β of the photofragments. Similarly Sugita et al. [13] reported an increase of the β value for the S atom from the OCS photodissociation. Recently, Larsen et al. [5] have demonstrated the control of the photodissociation branching ratio of I_2 that was aligned by a non-resonant intense laser pulse at 1.06 μm. In this Letter we demonstrate the same control method for the photodissociation branching ratio of Cl_2. When Cl_2 is irradiated at 404 nm, it is either excited to the $B^3\Pi_u^+(0_u^+)$ state that dissociates into $Cl + Cl^*$, or to the $^1\Pi_u(1_u)$ state that dissociates into $Cl + Cl$, where $Cl(3p^5{}^2P_{3/2})$ and

* Corresponding author. Fax: +81-75-753-5526.
E-mail address: mkawasa7@ip.media.kyoto-u.ac.jp (M. Kawasaki).
[1] Present address. Research Laboratory, Hitachi Chemical Co. Ltd., Tsukuba 300-4247, Japan.

0009-2614/01/$ - see front matter
PII: S0009-2614(01)00388-8

$Cl^*(3p^5{}^2P_{1/2})$ states are denoted by Cl and Cl^*, respectively. $Cl_2(B^3\Pi_u^+)$ is connected to the ground $X^1\Sigma_g(0_g^+)$ with a parallel transition moment, whereas the transition moment to $^1\Pi_u$ is perpendicular [14,15]. With Cl_2 aligned by non-resonant IR laser pulse, images of photofragment Cl were measured as a function of the IR laser intensity. Relatively weak IR field intensity allows us to discuss a quantitative relation between experimentally observed angular anisotropy parameter of the photofragment and the branching ratio of the Cl_2 photodissociation.

2. Experimental

A pulsed YAG pumped dye laser (5 ns, 2.5 mJ/pulse, 1 mm radius, 10 Hz) at 404.17 nm was used to dissociate Cl_2 and to ionize the Cl photofragment by $(3+1)$ resonance-enhanced multiphoton ionization (REMPI) in one-color laser scheme:

$$Cl(3p^5{}^2P_{3/2}) + 3h\nu\ (404.17\ \text{nm}) \rightarrow Cl(4s^1{}^2P_{3/2}),$$
$$Cl(4s^1{}^2P_{3/2}) + h\nu\ (404.17\ \text{nm}) \rightarrow Cl^+(3p^4).$$

The 1064 nm fundamental of the Nd^{3+}:YAG laser (1–15 mJ/pulse, 3 mm radius) was used to align the parent molecule prior to dissociation. The UV and IR laser beams were counter-propagated into the interaction region. Each laser was focused with a lens ($f = 0.20$ m) on a pulsed molecular beam of Cl_2 that was diluted in Ar (5%, backing pressure = 900 Torr). The IR beam diameter was larger than the UV laser diameter.

The REMPI signals of the chlorine atoms produced by the 404 nm dye laser were detected by velocity map imaging [16,17]. Briefly, the ions were focused onto a microchannel plate (MCP) mounted on the end of a 55 cm long flight tube. Electrons ejected from the rear plate of the MCP created an image on a phosphor screen. The image was recorded by a CCD camera and accumulated in a computer. The experimentally observed images were back-projected by a method similar to that used in computerized tomography [18]. The apparent angular anisotropy parameter, β, was obtained by a least squares fit of the 3D slice to the angular distribution function,

$$I(\theta) = A\left\{1 + \sum \beta_{2n} P_{2n}(\cos\theta)\right\}, \quad (1)$$

where $I(\theta)$ is the normalized angular distribution of the Cl photofragment, θ is the angle between the velocity of the Cl fragment and the electric vector of the dissociation laser beam, and $P_{2n}(x)$ is the $2n$-th Legendre polynomial.

3. Results

When Cl_2 absorbs a photon at 404 nm, it dissociates through either the parallel or perpendicular transitions:

$$Cl_2(X^1\Sigma_g, \Omega = 0) + h\nu\ (404.17\ \text{nm})$$
$$\rightarrow Cl_2(B^3\Pi_u^+, \Omega = 0) \rightarrow Cl + Cl^* \quad \text{(I)}$$
$$\rightarrow Cl_2(^1\Pi_u, \Omega = 1) \rightarrow Cl + Cl \quad \text{(II)}$$

The inset of Fig. 1 shows a typical image for the Cl photofragment, which consists of two rings since Cl and Cl^* are energetically separated by the spin–orbit splitting, $\Delta E_{so} = 0.109$ eV. The inner ring with kinetic energy of 0.24 eV corresponds to channel (I) and the outer one with 0.30 eV to channel (II). When a molecule is placed in an electric field of a pulsed IR laser, it can be aligned because of the anisotropy of its polarizability tensor. The alignment of the ground state Cl_2 by intense non-resonant IR laser pulses is demonstrated by change of the anisotropy of the photofragments. When the UV and IR lasers are parallel polarized, the β_2 value of the parallel channel (I) should increase because the parent Cl_2 molecules are aligned along the IR laser polarization axis. Careful examination of the image indicates that the image actually consists of three rings. The outermost ring is weak and not so well-resolved within our velocity resolution. Samartzis et al. [14] reported that the additional peaks in the velocity distribution that appear at the high-velocity side of the two main peaks correspond to 'hot band' dissociation of $Cl_2(v = 1)$. After Monte Carlo simulation for the kinetic energy distributions, they estimated the contribution of the hot bands to determine the branching ratios for the Cl_2 photodissociation at 310–470 nm. Samartzis et al. achieved a more accurate determination of the

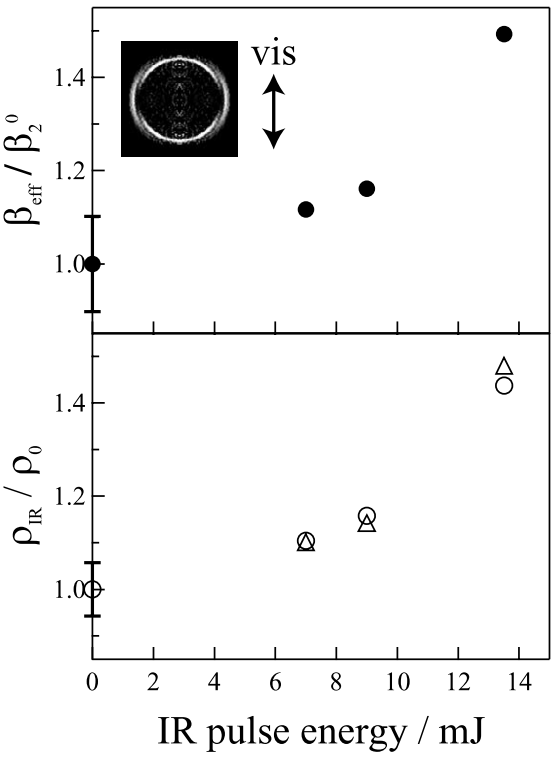

Fig. 1. Upper panel: change of the anisotropy parameter ratio $\beta_{\text{eff}}/\beta_2^0$ with 1.064 μm laser intensity for the $Cl(^2P_{3/2})$ photofragment. $Cl(^2P_{3/2})$ is produced from the $Cl(^2P_{3/2}) + Cl^*(^2P_{1/2})$ channel (I) of the 404 nm photodissociation of Cl_2. β_2^0 Is the averaged β_2 over several runs without IR laser. The inset shows an image of the Cl photofragments. The UV dissociating and IR aligning lasers have parallel polarizations. Lower panel: change of the branching ratio ρ_{IR}/ρ_0 with 1.064 μm IR laser intensity for channels (I) and (II). $\rho_{IR}/\rho_0 = [\Phi_\parallel/\Phi_\perp]_{IR}/[\Phi_\parallel/\Phi_\perp]_0$. Open circles – observed ratio; open triangles – calculated ratio from Eqs. (7) and (9).

ratios than ours because our velocity resolution is not enough to resolve the contribution of the hot bands. Hence, we adopt their value for the $\Phi_|/\Phi_\perp$ branching ratio at 404 nm, where $\Phi_|$ and $\Phi_\perp$ are the quantum yields of channel (I) and (II), respectively. Their branching ratio without the IR laser pulse is $\Phi_|/\Phi_\perp = 2.0 \pm 0.1$ at 404 nm from [14, Fig. 4]. Using this ratio for calibration purpose, we estimated the contribution of the hot bands in our images. Thus, the branching ratios at various IR aligning laser intensities are normalized to that in the absence of the IR laser, $\rho_{IR}/\rho_0 = [\Phi_|/\Phi_\perp]_{IR}/[\Phi_|/\Phi_\perp]_0$, which are shown in the lower panel of Fig. 1. When the IR laser intensity increased from 0 to 14 mJ, the ρ_{IR}/ρ_0 ratios increased from unity to 1.4. The ρ_{IR}/ρ_0 ratio was controlled only when the timing between visible and IR light was simultaneous. No appreciable changes were observed in the center-of-mass energy distribution with and without IR laser pulse.

The experimental angular distribution is a function of both the alignment due to an aligned m_J-state distribution of $Cl(^2P_{3/2})$ and the molecular alignment of the ground state Cl_2 due to the nonresonant IR laser field. The angular distribution for the aligned $Cl(^2P_{3/2})$ is effectively described by an expansion of Eq. (1) terminated at the fourth-order Legendre polynomial [14,19,20]. Samartzis et al. [14] reported that the angular parameters were $\beta_2 = 1.82$ and $\beta_4 = -0.24$. The contribution of the P_4 term is small partly because the precession time ($\sim$10 ns) of the total angular momentum J due to the hyperfine coupling ($\boldsymbol{F} = \boldsymbol{I} + \boldsymbol{J}$) with the nuclear angular momentum $\boldsymbol{I}$ is comparable to the pulse duration of the Nd:YAG pumped dye laser. The precession time is determined by the hyperfine coupling constant for an isolated free ^{35}Cl atom, $eqQ(^{35}Cl) = -110$ MHz [21]. Hence the degree of the m_J-state alignment can be reduced on average by a factor of three. Because our imaging data are congested by the contribution of the hot band and may not be reliable for analysis of the higher P_n terms that contribute to a small portion, the P_4 term was not included in Eq. (1) for our analysis of the angular distributions. In other words, we assumed that the angular distribution for the $Cl(^2P_{3/2})$ photofragment without the molecular alignment is described by an expansion of Eq. (1) terminated at the $P_2(\cos\theta)$ term. As will be discussed below, the molecular alignment is also expanded by the second-order Legendre polynomial when the IR laser field intensity is low. Combination of the two angular distributions results in an expansion terminated to the fourth-order Legendre polynomial. Thus, we analyzed our data for the photofragment angular distribution with an expansion terminated at the fourth-order Legendre polynomial. The upper panel of Fig. 1 shows the anisotropy parameter β_2 of the inner ring Cl atom for the parallel transition of Cl_2. The absolute value for the fragment anisotropy parameter in the

absence of the IR laser field, (β_2^0), is 1.4 ± 0.2. This value is smaller than the value of 1.82 reported by Samartzis et al. [14]. In the presence of the non-resonant IR laser field, the degree of alignment of the parent molecule increased. As shown in the upper panel of Fig. 1, the ratio $\beta_{\text{eff}}/\beta_2^0$ increased from unity to 1.5 at 14 mJ of the IR laser intensity where β_{eff} is the observed anisotropy parameter for $P_2(\cos\theta)$ in the presence of the IR laser field.

4. Discussion

4.1. Adiabaticity of Cl_2 potential curves

The Hamiltonian for the diatomic molecule is written as follows:

$$H(R) = H_{\text{elec}}(R) + T_{\text{nuc}}(R) + H_{\text{so}}(R), \tag{2}$$

where $H_{\text{elec}}(R)$ is a sum of an electronic Hamiltonian, $T_{\text{nuc}}(R)$ is a nuclear kinetic energy term, and $H_{\text{so}}(R)$ is the spin–orbit coupling. All these terms are functions of the nuclear distance R. In the adiabatic approximation, potentials are diagonalized with $H_{\text{elec}}(R) + H_{\text{so}}(R)$. Therefore, the nuclear kinetic energy operator gives rise to non-adiabatic interaction on the adiabatic potentials, which is written as follows [22]:

$$T_{\text{nuc}}(R) = -(h^2/8\pi^2\mu R)(\partial^2/\partial R^2)R + (h^2/4\pi^2\mu R^2)\boldsymbol{l}^2, \tag{3}$$

where $\boldsymbol{l}(= \boldsymbol{J} - \boldsymbol{L} - \boldsymbol{S})$ is the orbital angular momentum operator for the nuclei. The second term of Eq. (3) is known as Coriolis coupling. One selection rule for couplings by the radial derivative operator, the first term of Eq. (3), is $\Delta\Omega = 0$ and $g \leftrightarrow g/u \leftrightarrow u$, while that for the Coriolis coupling is $\Delta\Omega = \pm 1$ and $g \leftrightarrow g/u \leftrightarrow u$. The $^1\Pi(1u)$ state has a crossing point with the $B^3\Pi(0_u^+)$ state during the bond breaking. The transition promoted by the Coriolis couplings could take place at that point. However, reported experimental results of the angular distribution parameters β_2 of the Cl and Cl^* photofragments from the photodissociation at ~400 nm are close to the limit values for the parallel and perpendicular transitions [14,15]. These results indicate that the adiabatic dissociations occur and that the non-adiabatic transition induced by the nuclear kinetic term at the crossing point is negligible. In addition, according to the lifetime measurements of the rovibronic levels in the $B^3\Pi(0_u^+)$ state near the crossing point with the repulsive $^1\Pi(1u)$ state which is located below the $Cl + Cl^*$ dissociation limit, the predissociation rates through $^1\Pi(1u)$ by the Coriolis couplings are slow even at high rotational levels or $k < 10^6$ s^{-1}. Irradiation of Cl_2 at 404 nm induces the direct photodissociation process above the dissociation limit; separating atoms pass the crossing point within $\sim 10^{-12}$ s. This direct-dissociative lifetime is much shorter than the predissociative lifetime caused by the Coriolis coupling. Thus, it is reasonable to assume that the photodissociation occurs via an adiabatic process. Hence, the molecular alignment of the parent Cl_2 molecules by non-resonant IR laser pulse can control the branching ratio between the Cl + Cl and $Cl + Cl^*$ channels.

4.2. Degree of alignment of Cl_2 and photodissociation branching ratios

Suppose that the angle between the electric fields of the dissociating and aligning lasers is χ, the distribution of molecular axes referred to the electric vector of the dissociating laser is obtained by using the spherical harmonic addition theorem and then averaging over azimuthal angle [9]:

$$P(\theta_s) = (1/4\pi)\{1 + \gamma P_2(\cos\chi P_2(\cos\theta_s)\}, \tag{4}$$

where θ_s is the angle between the principle axis of the polarizability tensor and the electric vector of the dissociating laser. The control parameter γ of the degree of alignment for linear molecules is

$$\gamma = -(\langle\alpha\rangle - \alpha_{zz})(E^2/2kT), \tag{5}$$

where $\langle\alpha\rangle$ is the mean polarizability, α_{zz} is the element of the polarizability tensor along the symmetry axis and E is the rms optical electric field. Those molecules that absorb light have an angular distribution given by

$$\begin{aligned} I(\theta_s) &= P(\theta_s)\{1 + \beta_2^0 P_2\cos(\theta_s)\} \\ &= \frac{1}{4\pi}\left[1 + \left\{\beta_2^0 + \gamma\left(1 + \frac{2}{7}\beta_2^0 + \frac{1}{5}(\beta_2^0)^2\right)\right\}\right. \\ &\quad \times P_2(\cos\chi)P_2(\cos\theta_s) \\ &\quad \left. + \frac{18}{35}\beta_2^0\gamma P_2(\cos\chi)P_4\cos(\theta_s)\right]. \end{aligned} \tag{6}$$

In this equation the angle θ in Eq. (1) is substituted by the angle θ_s because the direction between the electric vectors of the alignment IR laser and the visible photodissociation laser is parallel, i.e. $\chi = 0$. Since the angular distribution of the photofragment is approximated by an expansion terminated at the $P_2(\cos\theta_s)$ term, the coefficient for the $P_2(\cos\theta_s)$ term of Eq. (6) is used for quantitative analysis of the degree of molecular alignment. Substituting $\chi = 0$ into Eq. (6), the observed control parameter γ is given by

$$\gamma = (\beta_{\text{eff}}/\beta_2^0 - 1)/(1/\beta_2^0 + 2/7 - \beta_2^0/5), \tag{7}$$

where β_{eff} is the observed anisotropy parameter for $P_2(\cos\theta_s)$ in Eq. (6). The cross-sections of the photodissociation processes from the aligned molecules are given by

$$\sigma_{\parallel}^{\text{align}} = 3\sigma_{\parallel}^0 \int_0^{2\pi} \int_0^{\pi} P(\theta_s)\cos^2\theta_s \sin\theta_s \,\mathrm{d}\theta_s \,\mathrm{d}\phi,$$

$$\sigma_{\perp}^{\text{align}} = \frac{3\sigma_{\perp}^0}{2} \int_0^{2\pi} \int_0^{\pi} P(\theta_s)\sin^2\theta_s \sin\theta_s \,\mathrm{d}\theta_s \,\mathrm{d}\phi, \tag{8}$$

where $\sigma_{\parallel}^0$ and $\sigma_{\perp}^0$ are cross-sections for photodissociation of non-aligned molecules, which are correlated to the parallel and perpendicular transition, respectively. From Eq. (8), ρ_{IR}/ρ_0 is given by

$$\rho_{\text{IR}}/\rho_0 = (5 + 2\gamma)/(5 - \gamma). \tag{9}$$

Substituting $\beta_{\text{eff}}/\beta_2^0$ of Fig. 1 and the value of β_2^0 of 1.4 into Eq. (7) and using Eq. (9), ρ_{IR}/ρ_0 is calculated as a function of IR laser intensity. The lower panel of Fig. 1 shows a good agreement between the calculated and experimental results.

For chlorine molecules $\langle\alpha\rangle = 4.61 \times 10^{-24}\text{cm}^3$ and $\alpha_{zz} = 6.60 \times 10^{-24}$ cm^3 [23,24]. The γ values of Eq. (5), which are calculated from Eq. (7), increase from 0 to 0.69 in the IR laser energy range 0–14 mJ. The value of the rms optical electric field is 9.3×10^6 V/cm or 1.1×10^{11} W/cm^2 at 14 mJ pulse energy, which is in agreement with our estimated value of 10^{10}–10^{11} W/cm^2. The average value of $\cos^2\Theta, \ll \cos^2\Theta \gg$, is $1/3 + 2\gamma/15$ where Θ is the angle between the principle axis of the polarizability tensor and the electric vector of the aligning laser. This value increases from 1/3 to $1/3 + 0.092$ for the energy range 0–14 mJ. In the experiments by Larsen et al. [5] and Sakai et al. [7], a larger increase was observed because their laser intensity was higher than ours.

Acknowledgements

This work is supported by a Grant-in-Aid in priority field 'Molecular Physical Chemistry'. Discussions with Prof. Richard Bersohn of Columbia University and Prof. Robert J. Gordon of the University of Illinois are appreciated.

References

[1] R.J. Gordon, S.A. Rice, Annu. Rev. Phys. Chem. 48 (1997) 601.
[2] C. Chen, Y.-Y. Yin, D.S. Elliot, Phys. Rev. Lett. 64 (1990) 507.
[3] L. Zhu, V. Kleiman, X. Li, S.P. Lu, K. Trentelman, R.J. Gordon, Science 270 (1995) 77.
[4] A. Assion, T. Baumert, M. Bergt, T. Brixner, B. Kiefer, V. Seyfried, M. Strehle, G. Gerber, Science 282 (1998) 919.
[5] J.J. Larsen, I. Wendt-Larsen, H. Stapelfeldt, Phys. Rev. Lett. 83 (1999) 1123.
[6] W. Kim, P.M. Felker, J. Chem. Phys. 104 (1996) 1147.
[7] H. Sakai, C.P. Safvan, J.J. Larsen, K.M. Hilligsoo, K. Hald, H. Stapelfeldt, J. Chem. Phys. 110 (1999) 10235.
[8] B. Friedrich, D.R. Herschbach, Phys. Rev. Lett. 74 (1995) 4623.
[9] A. Sugita, M. Mashino, M. Kawasaki, Y. Matsumi, R.J. Gordon, R. Bersohn, J. Chem. Phys. 112 (2000) 2164.
[10] L.G. Bakker, D.H. Parker, P.C. Samartzis, T.N. Kitsopoulos, J. Chem. Phys. 112 (2000) 5654.
[11] L.G. Bakker, D.H. Parker, P.C. Samartzis, T.N. Kitsopoulos, J. Chem. Phys. 113 (2000) 9044.
[12] P.C. Samartzis, B.L.G. Bakker, D.H. Parker, T.N. Kitsopoulos, J. Phys. Chem. A 103 (1999) 6106.
[13] A. Sugita, M. Mashino, M. Kawasaki, Y. Matsumi, R. Bersohn, G. Trott-Kriegeskorte, K.-H. Gericke, J. Chem. Phys. 112 (2000) 7095.
[14] P.C. Samartzis, B.L.G. Bakker, T.P. Rakitzis, D.H. Parker, T.N. Kitsopoulos, J. Chem. Phys. 110 (1999) 5201.
[15] Y. Matsumi, K. Tonokura, M. Kawasaki, J. Chem. Phys. 97 (1992) 1065.
[16] D.W. Chandler, P.L. Houston, J. Chem. Phys. 87 (1987) 1445.
[17] A.T.J.B. Eppink, D.H. Parker, Rev. Sci. Instrum. 68 (1997) 3477.
[18] Y. Sato, Y. Matsumi, M. Kawasaki, K. Tsukiyama, R. Bersohn, J. Phys. Chem. 99 (1995) 16307.

[19] Y. Wang, H.-P. Loock, J.-Y. Cao, C.X.W. Qian, J. Chem. Phys. 102 (1995) 808.
[20] A.S. Bracker, E.R. Woulters, A.G. Suits, Y.T. Lee, O.S. Vasyuitinskii, Phys. Rev. Lett. 80 (1998) 1626.
[21] R.N. Zare, Angular Momentum, Wiley, New York, 1988, p. 239.
[22] S.J. Singer, K.F. Freed, Y.B. Band, Adv. Chem. Phys. 61 (1985) 1.
[23] Landolt-Bölnstein, 6 Aufl., I band III, Springer, Berlin, 1951.
[24] J.O. Hirschfelder, C.F. Curtiss, R.B. Bird, Molecular Theory of Gases and liquids, Wiley, New York, 1963.